Mapping woodwind playability using measurement based physical models

Champ C. Darabundit; Vasileios Chatziioannou ⓘ ; Gary Scavone

Check for updates

View Online

Export Citation

International Symposium on Music and Room Acoustics

Loyola University
New Orleans, Louisiana

24-28 May 2025

Musical Acoustics

Mapping woodwind playability using measurement based physical models

Champ C. Darabundit

Department of Music Research, McGill University, Montreal, Quebec, H3A 1B9, CANADA; champ.darabundit@mail.mcgill.ca

Vasileios Chatziioannou

Department of Music Acoustics, University of Music and Performing Arts Vienna: Universitat fur Musik und darstellende Kunst Wien, Vienna, 1030, AUSTRIA; chatziioannou@mdw.ac.at

Gary Scavone

Department of Music Research, McGill University, Montreal, Quebec, H3A 1B9, CANADA; gary.scavone@mcgill.ca

Playability diagrams can provide insight into the behavior of a musical instrument under different playing conditions by visualizing the interaction between various musician-controlled playing parameters and their effects on the instrument's sound. These diagrams are created using measurements of real instruments or physics-based simulations. Recently, there has been an interest in producing playability diagrams of single-reed woodwind instruments using physical models. Our study furthers this exploration by using measured woodwind impedances and mouthpiece geometries to synthesize realistic instrument tones. By analyzing these tones, we aim to characterize the effects of different mouthpieces and instrument responses on playability and tone quality.

01 October 2025 13:32:40

1.   INTRODUCTION

In musical acoustics, playability maps are a common tool for evaluating the relationship between player controlled playing parameters and sound production in an instrument. These diagrams typically indicate regions where sound production is possible and locations of different oscillatory regimes. A common playability map used in the analysis of bowed string instrumented is the Schelleng diagram.[1] The Schelleng diagram demonstrates how various combinations of bow force and position result in distinct playing conditions. While the Schelleng diagram is derived from a simple analytical model, playability maps can also be constructed from measurements[2] or through physics-based simulations.[3]

Recently, there has been an increased interest in generating simulated playability maps for single-reed woodwind instruments.[4–6] These playability maps have been generated based on a lumped reed model that models the displacement of the reed tip. Single-reed woodwind playability maps utilize either a pressure-gap (p_m vs. y_0) map[4,5] or a pressure-stiffness (p_m vs. k) map.[6] Almeida et al.[7] experimentally measured playability by comparing pressure to lip force. As lip force is not a parameter in the lumped reed model, the pressure-gap and pressure-stiffness maps are substitutes for the pressure-lip force playability map.

In this paper, a simulated playability study is conducted using a lumped reed model with measured alto saxophone impedance responses and mouthpiece geometries. The aim of this study is to quantitatively compare the effects of different mouthpieces and measured impedance responses using simulated playability maps. A comparison is also made between pressure-gap and pressure-stiffness maps. In Section 2, the simulation study is further elaborated on. In Section 3, a new evaluation criteria is proposed and an initial comparison between pressure-gap and pressure-stiffness maps is presented. Section 4 presents results comparing the effects of different mouthpieces and different notes across the saxophone's range. Section 5 provides concluding remarks and avenues for future work.

2.   PLAYABILITY MAP GENERATION

The following physics-based model[8] is used to generate the playability maps shown in this paper. The reed is modeled in a lumped fashion,[9]

$$m\frac{d^2y}{dt^2} + m\gamma\frac{dy}{dt} + ky + f_c = S_r p_\Delta, \quad p_\Delta = p_m - p_b, \tag{1}$$

which models the displacement, y, of only the tip of the reed. m, γ, and k are the effective mass, damping, and stiffness of the reed tip. S_r is the effective reed area, and p_Δ is the pressure difference across the reed channel where p_m is the mouth pressure supplied by the player and p_b is the pressure inside the instrument. In the model presented here, y is offset by the initial reed gap, y_0, such that the equilibrium position of the reed is $y = 0$ and the mouthpiece boundary is located at y_0. The contact force, f_c is defined as

$$k_c[y - y_c]_+^\alpha \left(1 + \gamma_c\frac{dy}{dt}\right), \tag{2}$$

where k_c is the contact stiffness, y_c is the point where the contact force begins to take effect, γ_c is the contact damping, and α is a geometric exponent controlling the nonlinearity of the contact force. The function $[\cdot]_+ = \max(\cdot, 0)$ ensures that the force only acts when $y \geq y_c$. The flow into the instrument is modeled as a combination of a simple quasi-static Bernoulli flow, u_f, and a reed pumping flow, u_r,

$$u_b = u_f + u_r = \text{sign}(p_\Delta) S_j\sqrt{\frac{2|p_\Delta|}{\rho}} + S_r\frac{dy}{dt}. \tag{3}$$

S_j is the jet area equal to $w[y_0 - y]_+$ and w the width of the reed. ρ is the density of air. The lumped reed model is said to beat when the reed channel closes, $S_j = 0$.

As the intent here is to compare computed playability maps for different mouthpiece geometries, the saxophone body and mouthpiece are modeled separately. The saxophone body, from the neck down, is represented by a modal characterization, with parameters estimated through an optimization procedure from input impedance measurements.[10] This is motivated by the fact that it is difficult to accurately model an entire saxophone based on its geometry alone. A modal impedance, with frequency response

$$\hat{Z}(\omega) = \sum_m^M \frac{g_m j\omega}{-\omega^2 + 2\zeta_m \omega_m j\omega + \omega_m^2}, \tag{4}$$
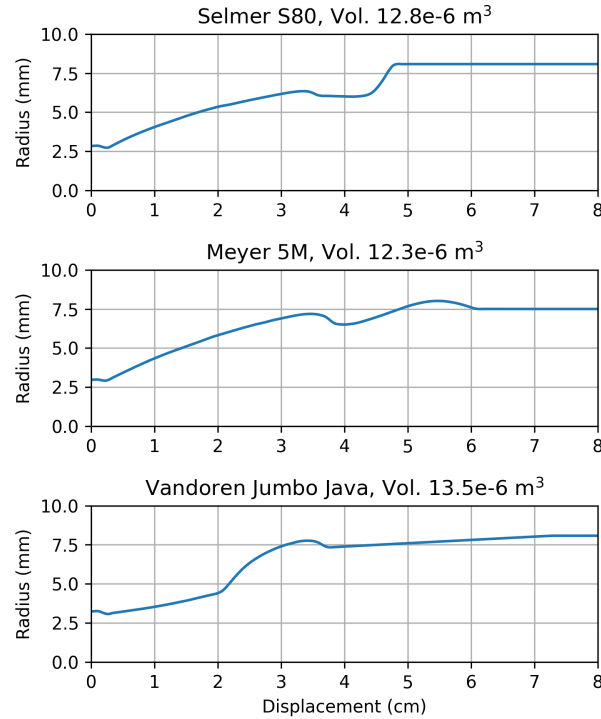
is used to ensure that the instrument impedance is positive real; a condition necessary for stable simulations. The system is composed of M modes with g_m, ζ_m, and ω_m the modal gain, damping, and frequency, respectively.

Wave propagation in the mouthpiece is modelled directly using the lossy horn equation.[8] Wave propagation in the absence of sideholes is reliably modelled using the lossy horn equation and the internal mouthpiece geometry is accurately inferred from the computed tomography (CT) scans of the mouthpiece. Furthermore, this approach reduces extraneous differences that might arise from estimating the modal parameters for multiple combined mouthpiece and body impedance responses. This ensures a fair comparison between mouthpiece geometries. The mouthpiece geometries were simplified to equivalent cylindrical areas which has been shown to accurately match the plane wave propagation in measured mouthpieces.[11] Three different mouthpieces, a Selmer S80, a Meyer 5M, and a Vandoren Java Jumbo, were evaluated with equivalent cylindrical geometries shown in Figure 1.

The static parameters used to generate the playability diagrams are given in Table 1. These parameters were chosen based on prior playability map studies for the clarinet[6] and scaling the values based on a slightly wider alto saxophone reed. All simulations were run at 192 kHz. A high audio sampling rate is necessary to capture the minute variations in area in the mouthpiece geometry. An alto saxophone was measured using a multi-microphone impedance head[12] across the entire range of the instrument. Modal parameters were estimated up to 12 kHz to avoid noise near the measurement device's cutoff frequency. For each combination of parameters, a 100 ms sample was generated, and a baseline analysis was carried out on the last 50 ms. To correctly tune the instrument, a length is subtracted from the end of the mouthpiece geometry (effectively pushing the mouthpiece further onto the instrument) until the first impedance peak coincides with the desired fundamental frequency. As in Chatziioannou et al., 2024,[6] if the resulting instrument pressure, p_b, is less than $1/6$ of the supplied blowing pressure, p_m, the note is considered unplayable and excluded from any further analysis. For notes that are above the pressure threshold, the fundamental frequency of each note is estimated with the pYIN algorithm.[13]

Table 1: Static parameters used in the synthesis. (p-s) and (p-g) refer to the parameters held constant in the pressure-stiffness and pressure-gap simulations.

Parameter	Value	Parameter	Value
m	10 mg	y_l (p-s)	1.2 mm
γ	8000 s^{-1}	y_c (p-s)	0.54 mm
α	2	k (p-g)	500 N/m
k_c	1.67 $\times 10^6$ N/m$^\alpha$		
γ_c	2 s/m		
w	13 mm		

01 October 2025 13:32:40

Figure 1: Mouthpiece geometries

3. EVALUATION METRICS

In his initial study, Woodhouse used both the deviation and harmonic number relative to the expected playing frequency as possible descriptors.[5] Other authors[6,7] have utilized the spectral centroid, as it is strongly correlated with the perception of brightness.[14] Colinot took a separate approach and classifies each note by the playing regime of the instrument.[4]

Figure 3 compares the stiffness-pressure map for a written G4 (233 Hz) using the spectral centroid and a proposed descriptor termed the harmonic band spectral centroid (HBSC). The HBSC analysis involves first defining the expected fundamental frequency, f_0. Then, a set of frequency bands with width f_0 with M frequency bins are established about the harmonics of the expected fundamental frequency kf_0, $k = 1, 2, \ldots K$. The HBSC descriptor is defined as

$$\text{HBSC} = \frac{\sum_{k=1}^{K} \left(\frac{1}{M} \sum_{m=-f_0/2}^{f_0/2} p\left(kf_0 + m\right) \right) f_k}{\sum_{k=0}^{K-1} \left(\frac{1}{M} \sum_{m=-f_0/2}^{f_0/2} p\left(kf_0 + m\right) \right)}, \tag{5}$$

where p is the magnitude response of the Fourier transform of the sample and f_k is the frequency corresponding to maximum magnitude in each respective band k,

$$f_k = \underset{f \in kf_0 + m}{\text{argmax}}\ p(f), \quad m = -f_0/2, \ldots, f_0. \tag{6}$$

K is the total number of harmonics considered. In the following plots, $K = 5$ was chosen. Inspired by the quasi-static regime analysis used by Colinot, 2020,[4] the HBSC is similar to the spectral centroid but focuses on the energy around the expected fundamental frequency of the instrument. The HBSC aims to visually provide hints regarding both the playing regime and the timbre quality of each note. A diagram of the descriptor is also shown in Figure 2.
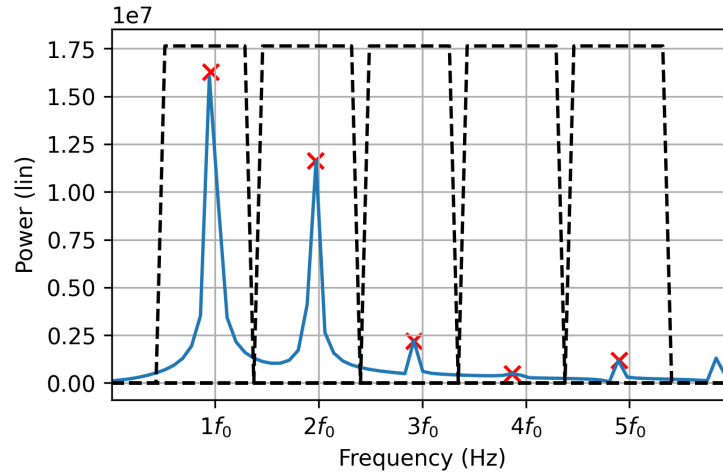
Figure 2: Diagram of the HBSC descriptor. The selected frequency bands of width f_0 centered around each harmonic kf_0 are shown in dashed lines. The selected peak frequency of each bin f_k is indicated by the red marker.

4.   RESULTS AND DISCUSSION
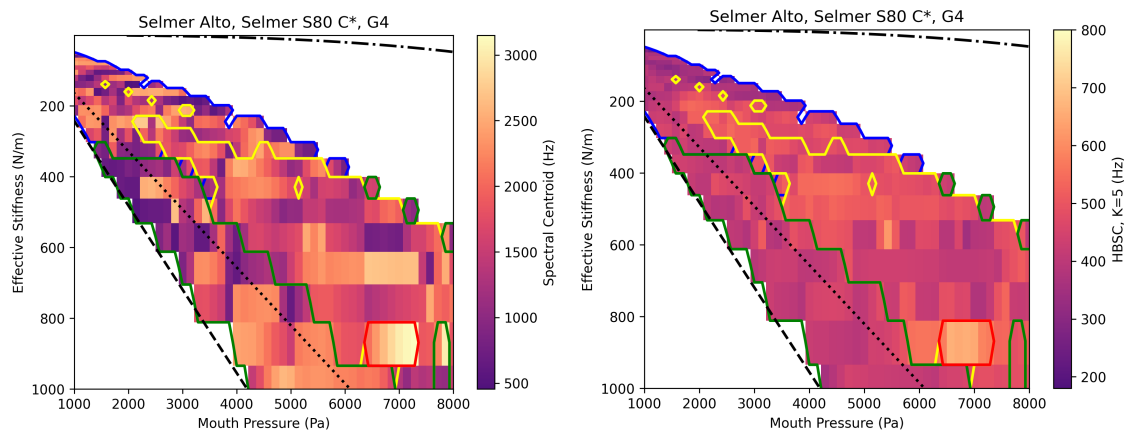
Figure 3: Pressure-stiffness map for an alto saxophone sounding a written G4. Included are the theoretical oscillation threshold (dashed), beating threshold (dotted), and saturation threshold (dashed dotted) from Dalpmt and Frappé.[15] Contour plot indicate areas of relative tuning to the expected sounding frequency. Blue: -1 octave to -1 semitone. Green: ± 1 semitone. Yellow: +1 semitone to +1 octave. Red: +1 octave and above.

Included in the playability maps are the theoretical oscillation, beating, and saturation thresholds for a simplified clarinet proposed by Dalmont and Frappé.[15] This simplified model considers a massless and undamped reed coupled to Raman's model of a cylinder. The equivalent length of the cylinder is chosen based on the expected fundamental frequency of the saxophone. Despite these simplifications, the theoretical oscillation and beating threshold were found to correlate well with behaviors seen in the numerical simulations. The saturation threshold does not correspond well to the simulated measurements. This is expected given the analysis for the oscillation threshold is based on the admittance of the first resonant frequency and the beating threshold is determined by the closure pressure of the reed. These thresholds are only weakly dependent on the impedance of the instrument. The saturation threshold, on the other hand, is
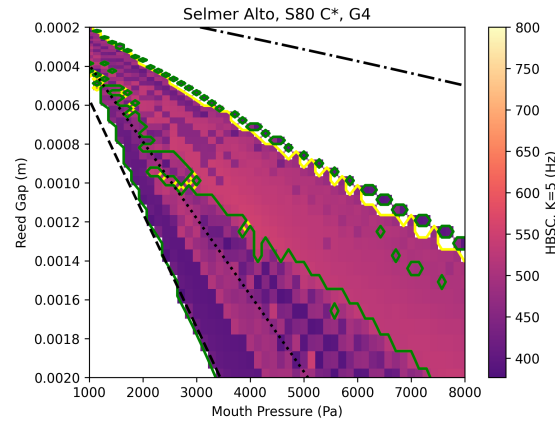
Figure 4: Pressure-gap map.

more dependent on the instrument's impedance.

The estimated sounding frequency, as determined by the pYIN algorithm, is overlaid on the playability map. The green region corresponds to estimated sounding frequency within ± 1 semitone of the desired fundamental. The blue region corresponds to frequencies from -1 octave to -1 semitone, the yellow region to frequencies from +1 semitone to 1 octave, and the red region to frequencies 1 octave and above.

For the pressure-stiffness maps, the effective stiffness per area was varied from 1 to 1000 N/m. The mouth pressure was varied from 1000 to 8000 kPa.

A.   HARMONIC SPECTRAL CENTROID

Some initial observation can be made about the pressure-stiffness maps in Fig. 3. In comparison to the spectral centroid descriptor, the HBSC provides a clearer view of the produced sound and corresponds well with the theoretical thresholds. Between the theoretical oscillation and beating thresholds, the HBSC value is low, and the instrument is sounding near the expected sounding frequency. For very low blowing pressures and stiffness coefficients, the instrument plays more than a semitone below its expected fundamental frequency, but not at the subharmonic. Above the beating threshold the instrument jumps to the next register and for very high pressure-low stiffness combinations, the instrument oscillates more than two octaves above the expected fundamental.

B.   PRESSURE-GAP VERSUS PRESSURE-STIFFNESS

A pressure-gap map is shown in Figure 4 using the HBSC descriptor. In lieu of a suitable predictor for the contact stiffness, the value was set to $y_c = 0.45 y_l$ based on the estimated parameters given by Chatziioannou et al., 2019.[9] The beating threshold again predicts the transition from playing near the fundamental to the next register. Compared to the pressure-stiffness diagram, the HBSC varies in a more predictable manner. As the collision stiffness is set arbitrarily, it is not clear if this response corresponds well to the behavior in a real instrument. For this reason, further analysis will be limited to pressure-stiffness maps.

C.   VARIATIONS BASED ON MOUTHPIECE RESPONSES

Figure 5 displays pressure-stiffness playability maps for a written G4 (233 Hz) for the Meyer 5M and Vanodren Jumbo Java mouthpieces. In comparison with the Selmer S80 response in Fig. 3, there are notable differences in the region above the theoretical beating threshold. In comparison to the Selmer S80 response in Figure 3, the Meyer 5M does not include a jump to the +1 octave region and has a more consistent HBSC
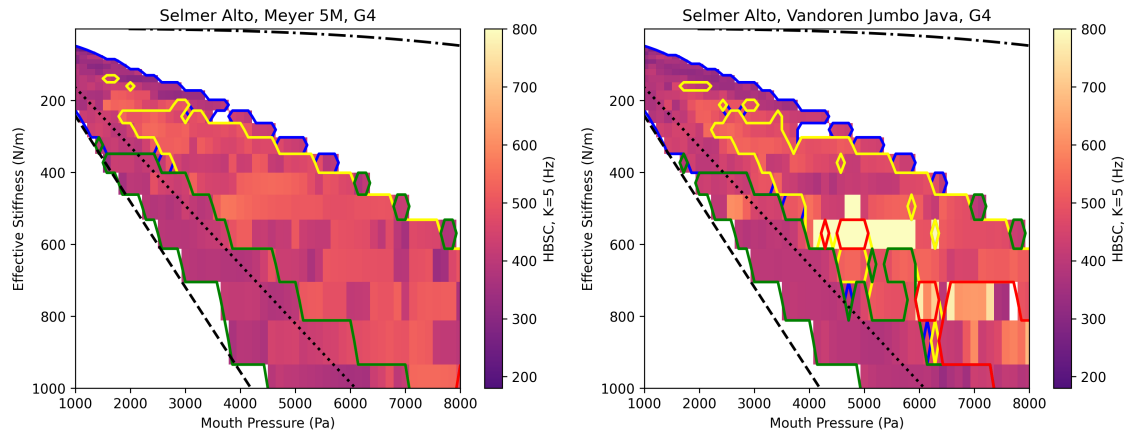
Figure 5: Playability maps for the Meyer 5M and Vandoren Jumbo Java mouthpieces

response overall. In contrast, the Vandoren Jumbo displays a larger variation in its HBSC response. Both mouthpieces are marketed as jazz mouthpieces.[16,17] The Vandoren Jumbo has a much lower baffle compared to the Meyer 5M and is known to have a much brighter sound. This is reflected in Fig. 5. The Selmer S80 mouthpiece is recommended for classical music.[18]
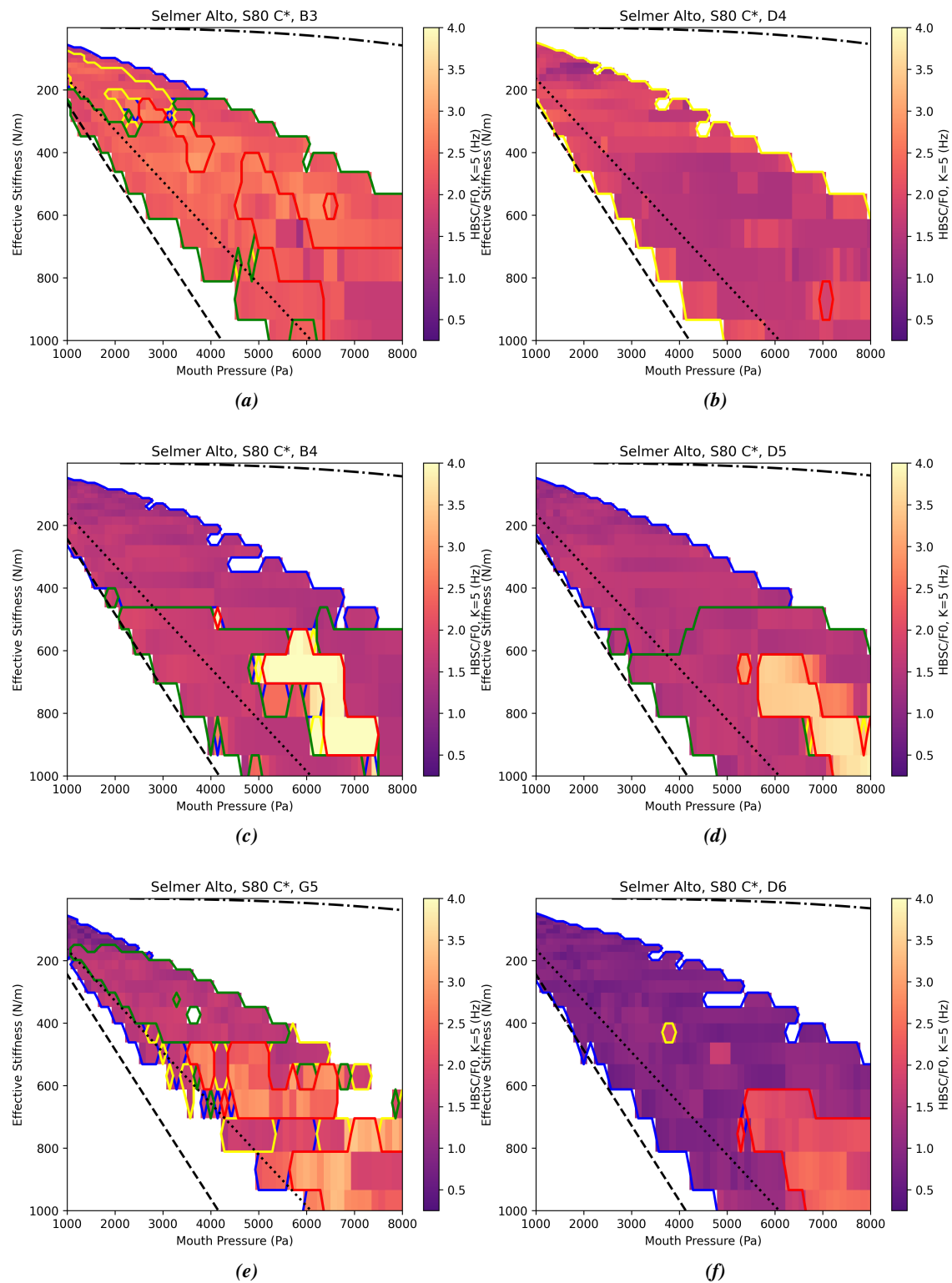
D.   VARIATION ACROSS THE RANGE OF THE INSTRUMENT

Figure 6 displays a pressure-stiffness maps across the range of the instrument for several notes. To evaluate the relative behavior for each note, the HBSC descriptor has been normalized by each note's expected fundamental frequency. Correspondingly, the scale is limited from 1/4 to 4 times the harmonic number. The mouthpiece position is based on tuning to the written G4 (233 Hz) note. No tuning adjustments were made for individual notes.

For the lowest evaluated note, B3, there is large region that sounds an octave higher, suggesting that it is easier to play up a register. For the highest evaluated note, D6, there is a lack of a fundamental frequency region. This suggests that the oscillations will tend to a lower regime for this note. It is possible that a different set of playing parameters, outside what is evaluated here, is necessary to sound the note effectively. It is also possible that correctly producing this note relies on vocal tract adjustments by the player.[19] This hypothesis is supported by evidence of vocal tract adjustments by clarinet players in regular playing of higher notes.[20]

For the notes B4 and B5, the flat (semitone below) region is relatively large and is at parameter combinations in D4 and G4 that play the fundamental. It is likely these notes will sound flat, suggesting that the mouthpiece needs to be adjusted to retune these notes. This must be done while balancing the tuning over the entire range. Generally, the beating threshold predicts some change in behavior for each playability map. However, the transition from the flat region to the fundamental region is not as clear as in the G4 playability map. A notable exception is D4, which plays sharp for the entire set of parameters.

01 October 2025 13:32:40

Figure 6: Pressure-stiffness playability maps for notes across the range of the instrument. Notes selected from a written G major chord, B5 is omitted for brevity.

5. CONCLUSION AND FUTURE WORK

In this paper, a preliminary study of simulated playability maps is presented based on measured instrument impedance responses and mouthpiece geometries. A descriptor termed the harmonic band spectral centroid is proposed whose aim is to provide information on both the playing regime of the instrument and timbre quality. A comparison between different mouthpiece geometries demonstrates how a mouthpiece's acoustic behavior affects the sound production in the instrument. This analysis is limited as the comparison does not take into account the mouthpiece lay geometry into the reed-lay interaction. Differences in lay geometry will affect parameters such as the reed effective stiffness, contact stiffness, and contact damping.

By simulating playability maps across the range of the instrument, it is possible to begin studying the variation in tone and playable regions for the entire instrument. Particularly, the movement of the fundamental frequency region could provide information regarding the ease of playability on the instrument. Large variations across different notes may suggest that the player has to make similarly large adjustments in their embouchure. This information could potentially be of interest to instrument makers looking to facilitate note transitions.

The parameters analyzed in this study can encapsulate the effects of more realistic playing parameters such as the player's embouchure, the mouthpiece's geometry, and the reed's hardness. However, they do not directly represent any, and it is likely that the player's embouchure effects both parameters. Future work could utilize a more intensive excitation mechanism model to study these other playing parameters. A recently proposed model[10] can incorporate the mouthpiece lay geometry in the simulation, thus providing a better comparison between different mouthpieces. To evaluate the accuracy of the simulated study, measurements are necessary. Future work could also include simulation of different instruments and looking at different audio descriptors such as note onset.

ACKNOWLEDGMENTS

REFERENCES

[1] J. C. Schelleng, "The bowed string and the player," *J. Acoust. Soc. Am.*, vol. 53, pp. 26–41, 1973.

[2] P. Galluzzo, *On the playability of stringed instruments*. PhD thesis, University of Cambridge, 2004.

[3] J. Woodhouse, "On the playability of violins. Part II: minimum bow force and transients," *Acustica*, vol. 78, pp. 137–153, 1993.

[4] T. Colinot, *Numerical simulation of woodwind dynamics: investigating nonlinear sound production behavior in saxophone-like instruments*. PhD thesis, Aix-Marseille Université (AMU), 2020.

[5] J. Woodhouse, "Mapping playability: The schelleng diagram and its relatives for bowed strings and wind instruments," in *Proc. Stockholm Music Acoust. Conf 2023*, 2023.

[6] V. Chatziioannou, M. Pàmies-Vilà, and A. Hofmann, "Physics-based playability maps for single-reed woodwind instruments," *JASA Express Lett.*, vol. 4, no. 3, p. 033201, 2024.

[7] A. Almeida, D. George, J. Smith, and J. Wolfe, "The clarinet: How blowing pressure, lip force, lip position and reed "hardness" affect pitch, sound level, and spectrum," *J. Acoust. Soc. Am.*, vol. 134, 2013.

[8] C. C. Darabundit and G. Scavone, "Discrete port-Hamiltonian system model of a single-reed woodwind instrument," *Front. Signal Process.*, vol. 5, 2025.

[9] V. Chatziioannou, S. Schmutzhard, M. Pàmies-Vilà, and A. Hofmann, "Investigating clarinet articulation using a physical model and an artificial blowing machine," *Acta Acustica united with Acustica*, vol. 105, pp. 682–694, 2019.

[10] C. C. Darabundit, V. Chatziioannou, and G. Scavone, "Distributed single-reed modeling based on energy quadratization and approximate modal expansion," in *Proc. 28th Int. Conf. Digital Audio Effects (DAFx25)*, accepted for publication.

[11] S. Wang, E. Maestre, and G. Scavone, "Acoustical modeling of the saxophone mouthpiece as a transfer matrix," *J. Acoust. Soc. Am*, vol. 149, pp. 1901–1912, 2021.

[12] S.-H. Jang and J.-G. Ih, "On the multiple microphone method for measuring in-duct acoustic properties in the presence of mean flow," *J. Acoust. Soc. Am.*, vol. 103, pp. 1520–1526, 1998.

[13] M. Mauch and Dixon, "pYIN: A fundamental frequency estimation using probabilistic threshold distributions," in *2014 IEEE Int. Conf. Acoust. Speech Signal Process. (ICASSP)*, 2014.

[14] J. M. Grey and J. W. Gordon, "Perceptual effects of spectral modifications on musical timbres," *J. Acoust. Soc. Am*, vol. 63, pp. 1493–1500, 1978.

[15] J.-P. Dalmont and C. Frappé, "Oscillation and extinction thresholds of the clarinet: Comparison of analytical results and experiments," *J. Acoust. Soc. Am.*, vol. 122, 2007.

[16] J. B. Company, "Meyer." online. https://www.jjbabbitt.com/meyer, date accessed: 04/20/25.

[17] V. Paris, "Saxophone mouthpieces." online. https://vandoren.fr/en/saxophone-mouthpieces/, date accessed: 04/20/25.

[18] H. S. Paris, "S80 mouthpiece for alto saxophone." online. https://www.selmer.fr/en/products/bec-s80-pour-saxophone-alto, date accessed: 04/20/25.

[19] G. Scavone, A. Lefebvre, and A. R. da Silva, "Measurement of vocal-tract influence during saxophone performance," *Journal of the Acoustical Society of America*, vol. 123, 2008.

[20] M. Pàmies-Vilà, A. Hofmann, and V. Chatziioannou, "The influence of the vocal tract on the attack transients in clarinet playing," *Journal of New Music Research*, vol. 49, no. 2, 2020.

01 October 2025 13:32:40